A moving-boundary formulation for modeling time-dependent two-phase flows

Eric W. Grald
Fluent Inc., Centerra Resource Park, Lebanon, NH, USA

J. Ward MacArthur
Honeywell Inc., Industrial Automation and Control, Phoenix, AZ, USA

A mathematical model describing the transient interactions in one-dimensional two-phase flows with heat transfer is presented. A moving-boundary refrigerant model is used to predict the position of the two-phase/vapor interface. A boundary immobilization technique is used to predict the temperature profile along the heat-exchanger wall. Typical results of an evaporator model, in terms of interface position and discharge superheat, are presented for inlet flow disturbances. The model is then used in an overall heat-pump simulation to predict cyclic performance. The results compare favorably to those obtained with a high-fidelity spatially dependent heat-pump model, but require significantly less computational effort.

Keywords: mathematical model; two-phase flow; moving boundary; evaporator; heat pump

Introduction

Generally, heat-exchanger models dealing with unsteady compressible two-phase flow fall into one of two categories: the lumped-parameter approach or the spatially distributed approach. MacArthur and Grald (1989) have previously developed a set of models in the latter category. In the previous work, the conservation equations are solved in an implicit fashion to yield unsteady profiles of temperature, enthalpy, density, flows, and mass. While the use of an implicit formulation allows integration time steps of up to ten seconds, the calculations are computationally intensive. Thus the spatially distributed model is not well suited for total system simulations (e.g., as part of a residential or commercial building simulation) in which there are many interacting components. It is therefore desired to construct a heat-exchanger model that will capture the essence of the spatially distributed model yet be significantly less costly.

Most existing transient heat-pump simulations described in the open literature utilize simplified heat-exchanger models in which spatial dependence is ignored. This includes the time-constant approach of Tree and Weiss (1986) and the single-node approach of both Dhar and Soedel (1979) and Chi and Didion (1982). James and James (1986) present a critical analysis and review of models for refrigeration systems and conclude that since 1973 the modeling approaches have been primarily based on stirred-tank representations of the heat exchangers.

The fundamental idea behind the moving-boundary approach presented here is to realize a decrease in computational complexity relative to the spatially distributed approach, while preserving a faithful representation of the heat-exchanger dynamic response. To accomplish this, the transition point concept first described by Wedekind (1965) has been extended. In this article, the spatial dependence of the heat exchanger is approximated by converting the governing partial differential equations of the compressible fluid into two ordinary differential equations. One is for determining the position of the two-phase/vapor interface, and the other is for determining the saturated vapor density, which can in turn be used to evaluate the pressure within the heat exchanger. In addition, the article presents a technique for accurately calculating the wall heat flux by a coordinate transformation that allows the spacing of the wall grid nodes to expand and contract as the two-phase/vapor interface moves.

Migration of refrigerant charge has been found to be one of the determining factors of dynamic heat-pump performance (Murphy and Goldschmidt 1982; Rasmussen et al. 1987). Any model must therefore have a means of representing the mass distribution. While this distribution is inherent in spatially distributed models, simplified approaches by their nature cannot be used to obtain this information. In the model to be described here, the distribution is incorporated by using mean void-fraction information, which is determined for a particular heat pump at various operating conditions from the mass profiles generated by the model described in MacArthur and Grald (1989).

The moving-boundary approach of the evaporator model was chosen to facilitate the investigation of refrigerant flow control strategies for which knowledge of the amount of superheat is required. The same moving-boundary approach can also be applied to the condenser, except that in the condenser there will be an additional interface: the two-phase/liquid interface. Since this analysis was primarily concerned with the evaporator, and hence with superheat

Address reprint requests to Dr. MacArthur at Honeywell Inc., Industrial Automation and Control, 16404 North Black Canyon Highway, Phoenix, AZ 85023, USA.

Received 5 October 1991; accepted 15 January 1992

response, less attention was focused on the condenser. The condenser was therefore treated in a more conventional lumped-parameter fashion. However, to maintain reasonable accuracy of the mass of refrigerant residing in the condenser, a functional parameter is introduced to ensure that the mean void fraction in the lumped-parameter model corresponds to that given by the spatially distributed model.

In the remainder of this article, attention will be focused on the moving-boundary approach used in the evaporator. Techniques for modeling the other components in a heat pump can be found throughout the literature (Erth 1970; Fischer and Rice 1981; Domanski 1982).

Governing equations

The transport processes taking place in the evaporator can be described mathematically by the governing conservation laws. If no approximations are made, the governing equations are the conservation of mass, momentum, and energy for a Newtonian fluid. These are a complex set of coupled, nonlinear partial differential equations. To maintain computational complexity at a reasonable level, a number of approximations are made:

- fluid flow is one-dimensional;
- viscous dissipation is negligible;
- spatial variations in pressure are negligible;
- axial conduction is negligible;
- work associated with the rate of change of pressure with respect to time is negligible;
- cross-sectional area of the flowstream is constant.

With these assumptions, the momentum equation is no longer necessary. The continuity and energy equations, respectively, become

$$\frac{\partial \rho A}{\partial t} + \frac{\partial \dot{m}}{\partial x} = 0 \tag{1}$$

$$\frac{\partial \rho A h}{\partial t} + \frac{\partial \dot{m} h}{\partial x} + H_r P_r (T_r - T_{hx}) = 0 \tag{2}$$

A more complete treatment of the derivation of Equations 1 and 2 is given in MacArthur and Grald (1989). These equations can be used to accurately predict the response of a heat exchanger with homogeneous flow in thermodynamic equilibrium. In most situations, the flow is not homogeneous due to the relative slip of the vapor and liquid phases. This phenomenon can be conveniently represented by a void-fraction model.

Evaporator model

All elements on the low-pressure side of the heat pump are encompassed in the evaporator model. In general, this includes the evaporator coil and the accumulator. The hermetic compressor sump, if one exists, can be combined with the accumulator. In this model, the accumulator is treated simply as a liquid mass storage node (its volume is included with the total low-side vapor volume). The rate of liquid flow from the accumulator is related to the compressor mass flow by a factor that is a fraction of the remaining liquid mass in the accumulator. This fraction is determined such that the accumulator "dries out" at the same time as the spatially distributed model (or experimental data) during a representative cycle. When the liquid falls below a certain level (i.e., below the j-tube), it is metered out at a constant fraction of the compressor mass flow rate.

The model for the evaporator coil itself can be developed from the basic conservation equations. To develop this model, consider the general situation depicted in Figure 1. As shown, the basic elements are the refrigerant, the heat-exchanger wall, and the secondary fluid. Each element of the model is described below.

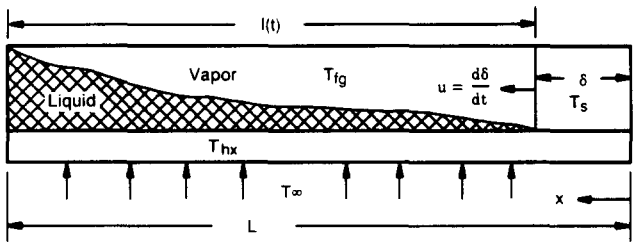

Figure 1 Schematic for model derivation

Notation

A	Cross-sectional or surface area
c_p	Specific heat
h	Enthalpy
H	Convective heat transfer coefficient
k	Thermal conductivity
l	Position of the two-phase/vapor interface
$\dot{m}$	Mass flow rate
N	Number of nodes in the heat-exchanger wall
P	Perimeter
q	Wall heat flux
Q	Heat flow in two-phase region
t	Time
T	Temperature
V	Total volume of evaporator, accumulator, and sump
x	Length coordinate
X	Refrigerant quality
α	Void fraction
δ	Length of superheat region
η	Dimensionless distance
ρ	Density

Subscripts

c	Compressor
f	Secondary fluid
fg	Latent
g	Saturated vapor
hx	Heat exchanger
i	Inlet
j	Node number
l	Saturated liquid
o	Outside
r	Refrigerant
xv	Expansion valve

Refrigerant

For the refrigerant, the basic conservation laws are given by Equations 1 and 2. It is convenient to first define the volume fraction of vapor relative to the total volume of the two-phase mixture at any flow cross section as the void fraction, α, and the unit wall heat flux as

$$q = H_r P_r (T_{hx} - T_r)$$

Equations 1 and 2 can then be written for the two-phase region as

$$\frac{\partial(\rho_l(1-\alpha)+\rho_g\alpha)A}{\partial t} + \frac{\partial \dot{m}}{\partial x} = 0 \tag{3}$$

$$\frac{\partial(\rho_l h_l(1-\alpha)+\rho_g h_g\alpha)A}{\partial t} + \frac{\partial \dot{m}(h_l + X h_{fg})}{\partial x} - q = 0 \tag{4}$$

It is now desired to obtain an expression for the position of the two-phase/vapor interface. To do so, first note that

$$h_l + X h_{fg} = h_g - (1-X)h_{fg}$$

Using this relationship, Equations 3 and 4 can be combined, expanded, and manipulated to give

$$\frac{\partial(\rho_l(1-\alpha)h_{fg}A)}{\partial t} - (\rho_l(1-\alpha)+\rho_g\alpha)A\frac{\partial h_g}{\partial t} + \frac{\partial(\dot{m}(1-X)h_{fg}}{\partial x} + q = 0 \tag{5}$$

In the first term of Equation 5, the variation of the latent heat of vaporization with respect to time is given by

$$\frac{\partial h_{fg}}{\partial t} = \frac{\partial h_{fg}}{\partial p}\frac{\partial p}{\partial t}$$

Assuming that the pressure dependence of the latent heat of vaporization is relatively small, this term can be neglected. Next, Equation 5 is integrated from the entrance of the evaporator to the two-phase interface, $l(t)$. This gives

$$\int_0^{l(t)} \frac{\partial}{\partial t}(\rho_l(1-\alpha)h_{fg}A)\,dx + \int_0^{l(t)} \frac{\partial}{\partial x}(\dot{m}(1-X)h_{fg})\,dx = -\int_0^{l(t)} q\,dx \tag{6}$$

The details of the integration of Equation (6) are given in the Appendix. If the variation of the refrigerant properties is assumed constant over the time step, then the expression for the two-phase/vapor interface becomes

$$\rho_l h_{fg} A(1-\bar{\alpha})\frac{dl}{dt} = -Q + \dot{m}_i(1-X_i)h_{fg} \tag{7}$$

where Q is the total heat transfer in the two-phase region and is an explicit function of $l(t)$. The continuity equation for the vapor and liquid phases, respectively, can be written by inspection from Equation 3. These expressions can then be integrated in a fashion similar to that of Equation 6. The continuity equation for the liquid phase becomes

$$A(1-\bar{\alpha})\rho_l\frac{dl}{dt} = (1-X_i)\dot{m}_i - \dot{m}_v \tag{8}$$

where the second term on the right-hand side of Equation 8 is the rate at which liquid refrigerant is converted to vapor along the length of the evaporator. The integrated form of the vapor continuity equation is

$$\bar{\alpha}A\frac{d\rho_g l}{dt} = (X\dot{m})_i + \dot{m}_v - \dot{m}_e \tag{9}$$

where the last term on the right-hand side of Equation 9 is the mass flow rate leaving the evaporator and entering the accumulator. This mass flow rate is determined in the accumulator model such that the boundary conditions required by the compressor are satisfied. By combining Equations 7 and 8, an expression for the vapor generation rate is given by

$$\dot{m}_v = \frac{Q}{h_{fg}}$$

Equation 9 can be modified by substituting the above expression, and by assuming that the vapor volume of the evaporator, accumulator, and sump, if one exists, is much larger than the liquid volume. This results in the following expression for the vapor density:

$$V\frac{d\rho_g}{dt} = (X\dot{m})_i + \frac{Q}{h_{fg}} - \dot{m}_e \tag{10}$$

where V is the total volume of the low-pressure side of the heat pump. Equation 7 can be used to predict the response of the two-phase/vapor interface, while Equation 10 can be used to determine the response of the vapor density. By assuming that this density is the saturated density and by using the equation of state for the refrigerant, the evaporator pressure can be determined in a straightforward fashion. Heat transfer in the two-phase region is given by Equation A7 (see Appendix). The heat transfer in the superheat region can be determined by performing an energy balance on the superheat section of the heat exchanger, the area of which is tentatively known. Integration of the heat flux requires information on the wall temperatures. A description of this model is given in the next section.

To complete the refrigerant model, information is required for the mean void fraction and on the liquid carryover (the amount of liquid initially drawn out of the evaporator by the compressor that is deposited in the accumulator) during the start-up transient. Correlations for these two quantities are obtained from results generated by the spatially distributed model described in MacArthur and Grald (1989). The void-fraction profile can then be integrated via Equation A3 in the Appendix to determine the mean void fraction at various operating conditions. For the particular evaporator results presented here, the mean void fraction was correlated well by a linear function of compressor speed. Typical values varied between 0.92 and 0.94. Liquid carryover is represented in the moving-boundary model by transferring a fraction of the liquid residing in the evaporator to the accumulator at the beginning of each start-up. As noted above, the amount of carryover is correlated to the results generated by the spatially distributed model.

Heat-exchanger wall

Including axial conduction, the heat transfer in the heat-exchanger wall is governed by the following form of the one-dimensional (1-D) energy equation:

$$(c_p\rho A)_{hx}\frac{\partial T_{hx}}{\partial t} = kA_{hx}\frac{\partial^2 T_{hx}}{\partial x^2} + H_o P_o(T_f - T_{hx}) - H_r P_r(T_{hx} - T_r) \tag{11}$$

Due to the movement of the two-phase/vapor interface, it is convenient to cast the energy equation in a suitable moving-boundary form. It is logical to treat the two-phase and superheat regions in a distinct fashion. To do this, it is necessary to properly account for the motion of the refrigerant interface adjacent to the wall. The approach taken here is a coordinate

transformation that in effect "freezes" the interface. In this frozen coordinate system, grids can be easily constructed for the temperature in both the two-phase and superheat regions. The accuracy of the solution for this approach is insensitive to the position of the interface. That is, the same number of grid elements is applied regardless of the interface position. For this transformation, the spatial direction is normalized relative to the interface, and the temperature becomes a function of the new coordinate as well as time. The transformation is given in terms of the following relationships:

$$\eta \equiv \frac{x}{\delta}$$

$$T \equiv T(\eta, t)$$

With these definitions, the derivatives in Equation 11 can be expanded. The temperature gradient becomes

$$\left.\frac{\partial T}{\partial x}\right|_t = \frac{\partial T}{\partial \eta}\left.\frac{\partial \eta}{\partial x}\right|_t + \frac{\partial T}{\partial t}\left.\frac{\partial t}{\partial x}\right|_t = \frac{1}{\delta}\frac{\partial T}{\partial \eta}$$

The second derivative of temperature with respect to distance becomes

$$\left.\frac{\partial^2 T}{\partial x^2}\right|_t = \frac{\partial}{\partial \eta}\frac{\partial \eta}{\partial x}\frac{1}{\delta}\frac{\partial T}{\partial \eta} = \frac{1}{\delta^2}\frac{\partial^2 T}{\partial \eta^2}$$

and the unsteady term becomes

$$\begin{aligned}\left.\frac{\partial T}{\partial t}\right|_x &= \frac{\partial T}{\partial \eta}\left.\frac{\partial \eta}{\partial t}\right|_x + \frac{\partial T}{\partial t}\left.\frac{\partial t}{\partial t}\right|_x \\ &= \frac{\partial T}{\partial \eta}\frac{d(x\delta^{-1})}{d\delta}\left.\frac{d\delta}{dt}\right|_x + \frac{\partial T}{\partial t} \\ &= -\frac{x}{\delta^2}\frac{d\delta}{dt}\frac{\partial T}{\partial \eta} + \frac{\partial T}{\partial t}\end{aligned}$$

Substituting these expressions into Equation 11 gives the following expression for the energy equation in transformed coordinates:

$$\begin{aligned}(c_p\rho A)_{hx}\frac{\partial T_{hx}}{\partial t} = (c_p A)_{hx}\frac{\eta}{\delta}\frac{d\delta}{dt}\frac{\partial T_{hx}}{\partial \eta} + \frac{(kA)_{hx}}{\delta^2}\frac{\partial^2 T_{hx}}{\partial \eta^2} \\ + H_o P_o(T_f - T_{hx}) - H_r P_r(T_{hx} - T_r) \qquad (12)\end{aligned}$$

The portions of the heat-exchanger wall adjacent to the two-phase and superheated refrigerant regions, respectively, are divided into a series of control volumes or nodes. Note that the orientation of x chosen here is positive in the direction opposite to the refrigerant flow. The discrete form of the energy equation can be obtained by integrating Equation 12 over a control volume from one control-volume face ("minus," labeled m) to the other ("plus," labeled p). This results in the following expression for the heat-exchanger wall:

$$\begin{aligned}\int_m^p (c_p\rho A)_{hx}\frac{\partial T_{hx}}{\partial t}\,d\eta = \int_m^p (c_p\rho A)\frac{\eta}{\delta}\frac{d\delta}{dt}\frac{\partial T_{hx}}{\partial \eta}\,d\eta \\ + \int_m^p \frac{(kA)_{hx}}{\delta^2}\frac{\partial}{\partial \eta}\frac{\partial T_{hx}}{\partial \eta}\,d\eta \\ + \int_m^p H_o P_o(T_f - T_{hx})\,d\eta \\ + \int_m^p H_r P_r(T_{hx} - T_r)\,d\eta \qquad (13)\end{aligned}$$

Assuming a linear temperature profile between nodes allows the following for use in evaluating Equation 13.

$$T_{hx,p} = \frac{(T_{hx,i+1} - T_{hx,i})}{2}$$

$$T_{hx,m} = \frac{(T_{hx,i} + T_{hx,i-1})}{2}$$

$$\left.\frac{\partial T_{hx}}{\partial \eta}\right|_p = \frac{(T_{hx,i+1} - T_{hx,i})}{\Delta\eta_p}$$

$$\left.\frac{\partial T_{hx}}{\partial \eta}\right|_m = \frac{(T_{hx,i} - T_{hx,i-1})}{\Delta\eta_m}$$

Thus the final form of Equation 13 becomes

$$\begin{aligned}\delta\Delta\eta_i(c_p\rho A)_{hx}\frac{dT_{hx,i}}{dt} \\ = (c_p\rho A)_{hx}\frac{\eta_i}{2}\frac{d\delta}{dt}(T_{hx,i+1} - T_{hx,i-1}) \\ + \frac{(kA)_{hx}}{\delta}\left[\frac{(T_{hx,i+1} - T_{hx,i})}{\Delta\eta_p} - \frac{(T_{hx,i} - T_{hx,i-1})}{\Delta\eta_m}\right] \\ + \delta\Delta\eta_i(H_o P_o(T_f - T_{hx,i}) - H_r P_r(T_{hx,i} - T_{r,i})) \qquad (14)\end{aligned}$$

where $i = 1$ to N nodes. A similar set of equations exists for both the two-phase and superheat sections of the heat exchanger.

Secondary fluid

The energy conservation equation for the incompressible secondary fluid is

$$(c_p\rho A)_f\frac{\partial T_f}{\partial t} + (\dot{m}c_p)_f\frac{\partial T_f}{\partial x} + H_o P_o(T_f - T_{hx}) = 0 \qquad (15)$$

where the mass flow-rate term is negative for counterflow applications and is uniform along the length of the heat exchanger. For parallel flow applications, the mass flow term is positive. To model crossflow situations, the equations must be modified to properly account for the number of passes.

Solution procedure

The evaporator equations are solved in an iterative fashion at each time step. First a guess for the evaporator pressure is made. The saturated refrigerant properties and inlet quality are then computed. The position of the two-phase/vapor interface is calculated via the implicit form of Equation 8. The total heat transfer in the two-phase region is then determined. A secant method is used to guess a new pressure. This procedure is repeated until the implicit form of Equation 10 is satisfied. The temperature profile in the superheated vapor can then be determined. Next the derivatives of the heat-exchanger wall and secondary-fluid temperatures are computed. The mass flow rates into and out of the accumulator, the enthalpy of the refrigerant leaving the accumulator, and the amount of liquid remaining in the accumulator are calculated last. Finally, the heat-exchanger wall and secondary-fluid derivatives are integrated and the time step is incremented.

Results

To illustrate the fundamental characteristics of the model, results will be presented for inlet flow disturbances.

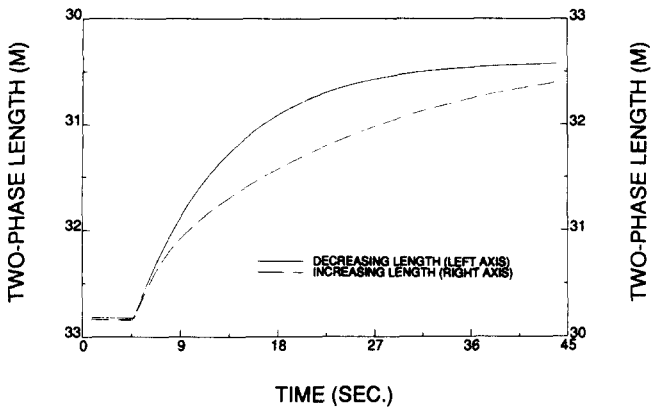

Figure 2 Transition-point response for step increase and decrease in inlet flow

Characteristic open-loop responses of both the two-phase/vapor interface and the exit superheat will be described. Next, the closed-loop performance of the model in an overall heat-pump simulation will be given. Heat-pump results with the moving-boundary model will be compared with results obtained using a detailed spatially dependent model.

Open-loop performance

A description of the physical interactions will be given to foster a better understanding of the results to be presented shortly. First, consider the case of constant evaporator pressure and uniform external heat flux along the heat-exchanger wall in which there is no thermal capacitance. Neglecting thermal capacitance implies that there will also be a uniform heat flux along the inner wall. A step decrease in refrigerant mass flow rate in this instance would reduce the length of the two-phase region. The difference between the initial and final position of the two-phase/vapor interface represents an excess of liquid that must be vaporized. Physically, the time constant for the interface to move from its initial to final position represents the time that would be required to vaporize all the excess liquid, provided that the heat transfer rate to the excess liquid was equal to the rate that existed at the beginning of the transient. Thus, theoretically, it takes an infinite amount of time to move from the initial to the final position. The reason is that the heat transfer rate to the excess liquid asymptotically approaches zero as the heat transfer area approaches zero.

A similar scenario exists for a step increase in flow when the thermal capacitance of the tube wall is neglected. In this instance, rather than having an initial excess of liquid, there will be an initial shortage of liquid. The response, however, will be the same, since the internal heat flux is uniform.

When the thermal capacitance of the tube wall is taken into account, the internal heat flux can be nonuniform and time dependent even when the external heat flux is maintained constant. This situation will exist when the two-phase/vapor interface moves in a direction where the temperature is higher than it would be under steady conditions. Thus the transient response will, in general, be different depending on whether the flow is increased or decreased.

To show the effect of inlet flow disturbances, the evaporator will be simulated in an open-loop fashion. For this test, evaporator pressure will be held constant at 690 kPa such that the evaporation temperature has no impact on the results. In addition, the inlet enthalpy is maintained at 103 kJ/kg and the dry-bulb/wet-bulb air temperature entering the coil is maintained at 27/20°C. Flow disturbances are introduced by either making a step increase in flow from 0.068 kg/s to 0.073 kg/s or by making a step decrease in flow from 0.073 kg/s to 0.068 kg/s.

Figure 2 shows the results of the model for a step increase and a step decrease in flow. The response of the two-phase/vapor interface clearly differs depending on whether the flow is increased or decreased. The right axis corresponds to an increasing flow (the two-phase length increases) while the left axis corresponds to a decreasing flow (the two-phase length decreases). As described above, the significant interaction with the tube wall occurs primarily when the interface encounters tube temperatures significantly higher than those that will exist under steady conditions. The effect of this interaction is to slow down the response and to distort the shape of the response curve. The receding interface exhibits classical exponential response and approximates the case for uniform heat flux. The discrepancy between the two curves increases as the tube capacitance increases.

Movement of the interface directly affects the amount of superheat that leaves the evaporator. Response of the two-phase interface and corresponding discharge superheat is illustrated in Figures 3 and 4 for a decrease and increase in flow, respectively. These results correspond directly to those of the previous figure, except that here the time base has been expanded to capture the complete response. Again, the characteristic response is substantially different depending on whether the flow is increased or decreased. As the flow is

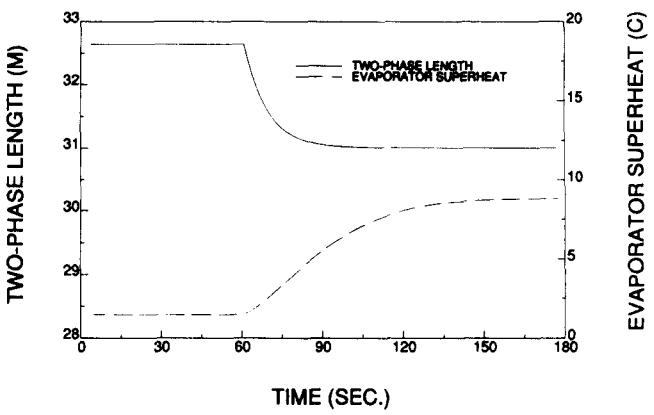

Figure 3 Two-phase length and superheat response for step decrease in inlet flow

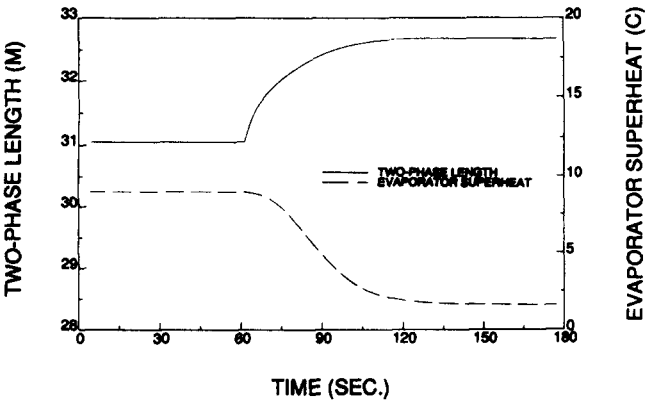

Figure 4 Two-phase length and superheat response for step increase in inlet flow

increased, the apparent order of the response increases relative to the case of decreasing flow. Unlike the interface response, the superheat response does not exhibit a maximum slope at the onset of the transient.

Closed-loop performance

In this section, attention is focused on the operation of the closed-loop system. The moving-boundary model is used only for the evaporator and is combined into an overall heat-pump simulation that includes gas engine, variable-speed compressor, condenser, and expansion-valve models. The simulation is run in both the cooling and heating modes. In the cooling mode, air enters the evaporator and condenser at 27°C and 30°C, respectively, and the compressor is run at low speed (1000 rpm). In the heating mode, air enters the evaporator and condenser at 8°C and 20°C, respectively, and again the compressor is run at low speed.

As described previously, the objective of the moving-boundary model is to reduce computational effort relative to that required by a spatially dependent model while preserving a faithful representation. The basis of comparison for the present study is the model described in MacArthur and Grald (1989). This model has been tested for various systems—air-to-air, water-to-water, open, and hermetic—under a variety of conditions, and has been compared to experimental data. An example of the performance of the spatially dependent model is given in Figure 5 (taken from MacArthur and Grald (1989), with permission), which shows a comparison between predicted and measured pressure responses.

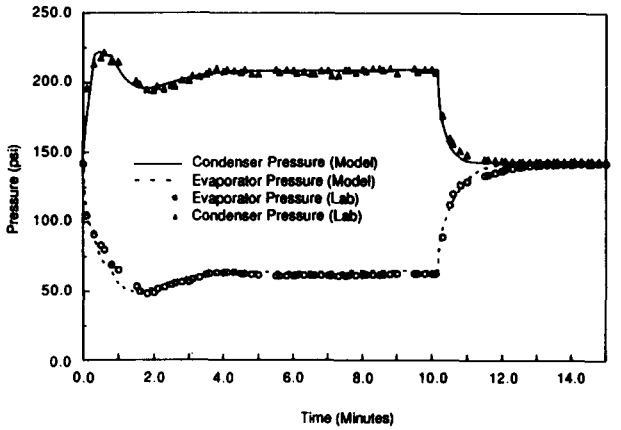

Figure 5 Pressure response for spatially distributed model and comparison with experimental data (from MacArthur and Grald (1989), with permission)

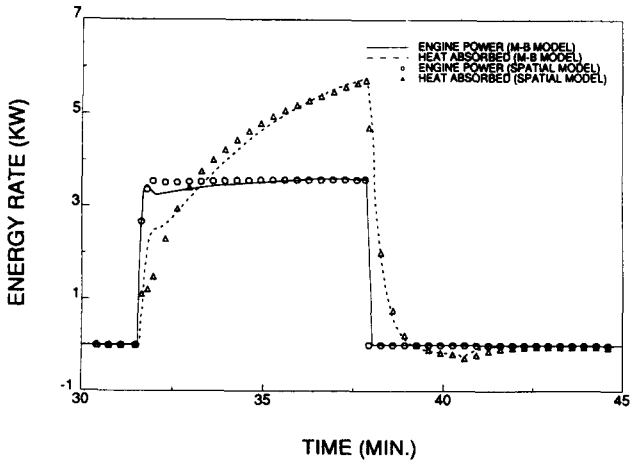

Figure 6 Comparison between moving-boundary and spatially dependent model (cooling mode)

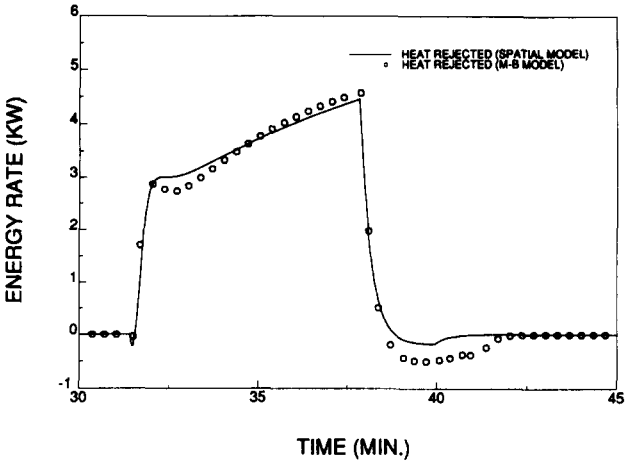

Figure 7 Comparison between moving-boundary and spatially dependent model (heating mode)

Although the performance of the spatial model has proved to be accurate, its usefulness has been limited by computational complexity. The moving-boundary approach presented here has resulted in an order-of-magnitude reduction in computational effort. Figure 6 illustrates that this reduction in effort has not come at the expense of accuracy in predicting evaporating response. This test was conducted in the cooling mode under the conditions described above. Experience has shown that the response of the heat pump is very sensitive to the interactions within the evaporator and accumulator. Therefore, only the evaporator was modeled using the moving-boundary approach. A lumped-node formulation was used to represent the condenser.

Even though the condenser model is very simple, Figure 7 shows that it is reasonably accurate at predicting heat rejected during the heating mode. This accuracy is a synergistic effect of using the moving-boundary model in the evaporator where it is most needed. The largest discrepancies occur during the off period, which is precisely when the evaporator has the least impact on condenser response. During the off period, the simplified model allows the condenser pressure to fall too far, and hence there is too much heat absorbed (negative heat rejected).

Conclusions

A moving-boundary model has been presented for predicting heat-exchanger response for two-phase flow applications. While the model was developed for evaporators used in heat pumps, the technique can be applied to heat exchangers in general with simple 1-D two-phase flows where pressure gradients and head terms are unimportant. The approach can result in significant computational savings relative to a spatially distributed model without substantial loss in accuracy. The approach does require a priori information on mean void fraction and is more complex than simple, single-node models. Since this technique captures the effect of direction of the two-phase interface on discharge temperature, it can be used to advantage in designing better discharge temperature controllers.

References

Chi, J. and Didion, D. (1982) A simulation of the transient performance of a heat pump. *Int. J. Refrig.*, **5**, 176–183

Dhar, M. and Soedel, W. (1979) Transient analysis of a vapor compression refrigeration system. *Proc. 25th Int. Cong. of Refrigeration*, Venice, Italy

Domanski, P. (1982) Computer modeling of the vapor compression cycle with constant flow area expansion device. Ph.D. thesis, School of Engineering and Architecture, Catholic University of America, Washington, DC

Erth, R. A. (1970) Two-phase flow in refrigeration capillary tubes: analysis and prediction. Ph.D. thesis, Mechanical Engineering Dept., Purdue University, West Lafayette, IN

Fischer, S. K. and Rice, C. K. (1981) A steady state computer design model for air-to-air heat pumps. ORNL/CON-80, Oak Ridge National Laboratory, Oak Ridge, TN

James, K. A. and James, R. W. (1986) A critical survey of dynamic mathematical models of refrigeration systems and heat pumps and their components. Technical Memorandum No. 97, Institute of Environmental Engineering, Polytechnic South Bank, London, UK

MacArthur, J. W. and Grald, E. W. (1989) Unsteady compressible two-phase flow model for predicting cyclic heat pump performance and a comparison with experimental data. *Int. J. Refrig.*, **12**, 29–41.

Murphy, W. E. and Goldschmidt, V. W. (1982) Cycling characteristics of a residential air conditioner-modeling of shutdown transients. *ASHRAE Trans.*, **92** (1), 186–202.

Rasmussen, R. W., MacArthur, J. W., Grald, E. W., and Nowakowski, G. A. (1987) Performance of engine-driven heat pumps under cycling conditions. *ASHRAE Trans.*, **93** (2), 1078–1090.

Tree, D. R. and Weiss, B. W. (1986) Two time constant modeling approach for residential heat pumps. Preprints of the 1986 International Institute of Refrigeration, 141–148

Wedekind, G. L. (1965) Transient response of the mixture-vapor transition point in two-phase horizontal evaporating flow. Ph.D. thesis, Mechanical Engineering Dept., University of Illinois, Urbana, IL

Appendix

Integration of Equation 6 requires correct treatment of the time-dependent integration limit. To treat this situation, Leibniz's rule is used. Hence, for the first term,

$$\int_0^{l(t)} \frac{\partial}{\partial t}(\rho_l(1-\alpha)h_{fg}A)dx = \frac{\partial}{\partial t}\int_0^{l(t)} \rho_l(1-\alpha)h_{fg}Adx - \rho_l(1-\alpha)h_{fg}A|_{x=l(t)}\frac{dl(t)}{dt} \quad \text{(A1)}$$

Since the density–enthalpy product is constant along the length of the heat exchanger, this term may be removed from the integral. At $x = l(t)$, the void fraction is unity; hence, one minus the void fraction is zero, and the last term in Equation A1 is zero. The above expression can therefore be written as

$$\int_0^{l(t)} \frac{\partial}{\partial t}(\rho_l(1-\alpha)h_{fg}A)dx = \frac{\partial}{\partial t}\left[\rho_l h_{fg}Al(t)\frac{1}{l(t)}\int_0^{l(t)}(1-\alpha)dx\right] \quad \text{(A2)}$$

By definition, the mean value of the void fraction is

$$\bar{\alpha} = \frac{1}{l(t)}\int_0^{l(t)} \alpha dx \quad \text{(A3)}$$

Therefore, Equation A2 becomes

$$\int_0^{l(t)} \frac{\partial}{\partial t}(\rho_l(1-\alpha)h_{fg}A)dx = \frac{\partial}{\partial t}\rho_l h_{fg}A(1-\bar{\alpha})l(t) \quad \text{(A4)}$$

Direct integration of the next term in Equation 6 gives

$$\int_0^{l(t)} \frac{\partial}{\partial x}\dot{m}(1-X)h_{fg}dx = \dot{m}(1-X)h_{fg}|_{x=l(t)} - \dot{m}(1-X)h_{fg}|_{x=0} \quad \text{(A5)}$$

Since the quality, X, at $x = l(t)$ is by definition unity, Equation A5 becomes

$$\int_0^{l(t)} \frac{\partial}{\partial x}\dot{m}(1-X)h_{fg}dx = -\dot{m}_i(1-X_i)h_{fg} \quad \text{(A6)}$$

where the subscript i refers to evaporator inlet conditions. The final term in Equation 6 is the total heat flow in the two-phase region. This term can be evaluated by

$$Q = \int_0^{l(t)} qdx \quad \text{(A7)}$$

Equations A4, A6, and A7 can be substituted into Equation 6 to give the response of the moving refrigerant boundary. Since the integrations remove the spatial dependence from the refrigerant problem, the partial differential equation is reduced to an ordinary differential equation.